A LC–Electrospray Tandem MS Method for the Analysis of Naltrexone in Canine Plasma Employing a Molecular Model to Demonstrate the Absence of Internal Standard Deuterium Isotope Effects

Sunil S. Iyer[1], Glen E. Kellogg[2], and **H. Thomas Karnes[1,*]**

[1]Department of Pharmaceutics, School of Pharmacy, Virginia Commonwealth University, Richmond, VA 23298-0533 and [2]Department of Medicinal Chemistry, School of Pharmacy & Institute for Structural Biology and Drug Discovery, Virginia Commonwealth University, Richmond, VA 23298-0540.

Abstract

A simple and sensitive method is described for the determination of naltrexone (NAL), an opioid antagonist, in dog plasma. Sample processing involved a single step liquid–liquid extraction, followed by evaporation of the supernatant, and reconstitution of the residue prior to injection into the liquid chromatograph. The peak height ratio of NAL to [15,15,16-^{2}H] naltrexone (NAL-d_3) was used for quantitation. Observation of the chromatograms for NAL and NAL-d_3 revealed that the mean retention times of the compounds were 1.32 and 1.31 min, respectively. The almost identical retention times possibly accounted for the absence of matrix effects influencing quantitation. Molecular mechanics calculations using SYBYL software were carried out to qualitatively and quantitatively assess analyte and isotopic internal standard stationary phase interactions. Binding energy values of –10.22 and –10.26 kcal/mole were obtained for NAL and NAL-d_3, respectively. These data predict, semi-quantitatively, the absence of deuterium isotope effects that may influence quantitation. Calibration curves were linear from 10 pg/mL to 5014 pg/mL with a weighting factor of 1/x. Precision and accuracy and reverse predicted concentration residuals were within 15%. The method has been used successfully for the analysis of plasma samples from a pilot subcutaneous implantation study in dog.

Introduction

Naltrexone (NAL), an opiate receptor antagonist, has been marketed as an oral tablet for the clinical management of opiate addiction and as adjunctive treatment for individuals with alcohol dependence (1–3). However, patient non-compliance to dosage schedules is a difficult obstacle to treatment. Two factors, namely, the complete abstinence of opioid-induced reinforcing effects and the absence of adverse consequences (unlike methadone) upon discontinuation of medication are primarily responsible for patient non-compliance (4). To overcome this problem, dosage forms such as implants and depots are under different stages of development in order to have a long-acting alternative to the tablet (5–7).

An early report on bioanalytical methods for NAL is available as a National Institute on Drug Abuse (NIDA) monograph (8). This report includes an electron-capture gas chromatographic (GC) assay, a gas-liquid chromatographic assay in different matrices, and a thin-layer chromatography (TLC) procedure described by Wall and Brine. These methods involved large sample volumes and complicated sample preparation techniques. The mid-90s saw the development of various methods on high-performance liquid chromatography (HPLC) with UV or amperometric detection (9–11).

In recent years, there is renewed interest among physicians in exploring treatments with low doses of NAL (12). In addition, through the use of a dual-detector system with positron-emitting radioactive drugs, Lee et al. (13) established that NAL had a significantly longer half-life due to receptor occupancy as compared to its estimated plasma half-life. This has promoted a larger number of pharmacokinetic studies that pose additional challenges to the analytical chemist to develop more sensitive and selective methods for quantitation. Publications on GC–mass spectrometry (MS) and liquid chromatography (LC)–mass spectrometry (MS)–MS for estimation of NAL and its major metabolite, 6β-naltrexol, in various biological matrices report lower limits of quantitation (LLOQ) in the range of 0.1–2 ng/mL (14–17). No report is available, how-

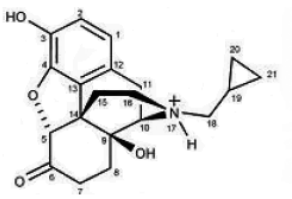

Figure 1. Naltrexone, protonated under acidic conditions.

*Author to whom correspondence should be addressed: email tom.karnes@vcu.edu..

Table I. Gradient Conditions for the Mobile Phase

Time (min)	Pump A (%)	Pump B (%)	Curve
0.10	5	95	0
1.25	100	0	1
2.50	100	0	0
2.51	5	95	0
3.00	5	95	0

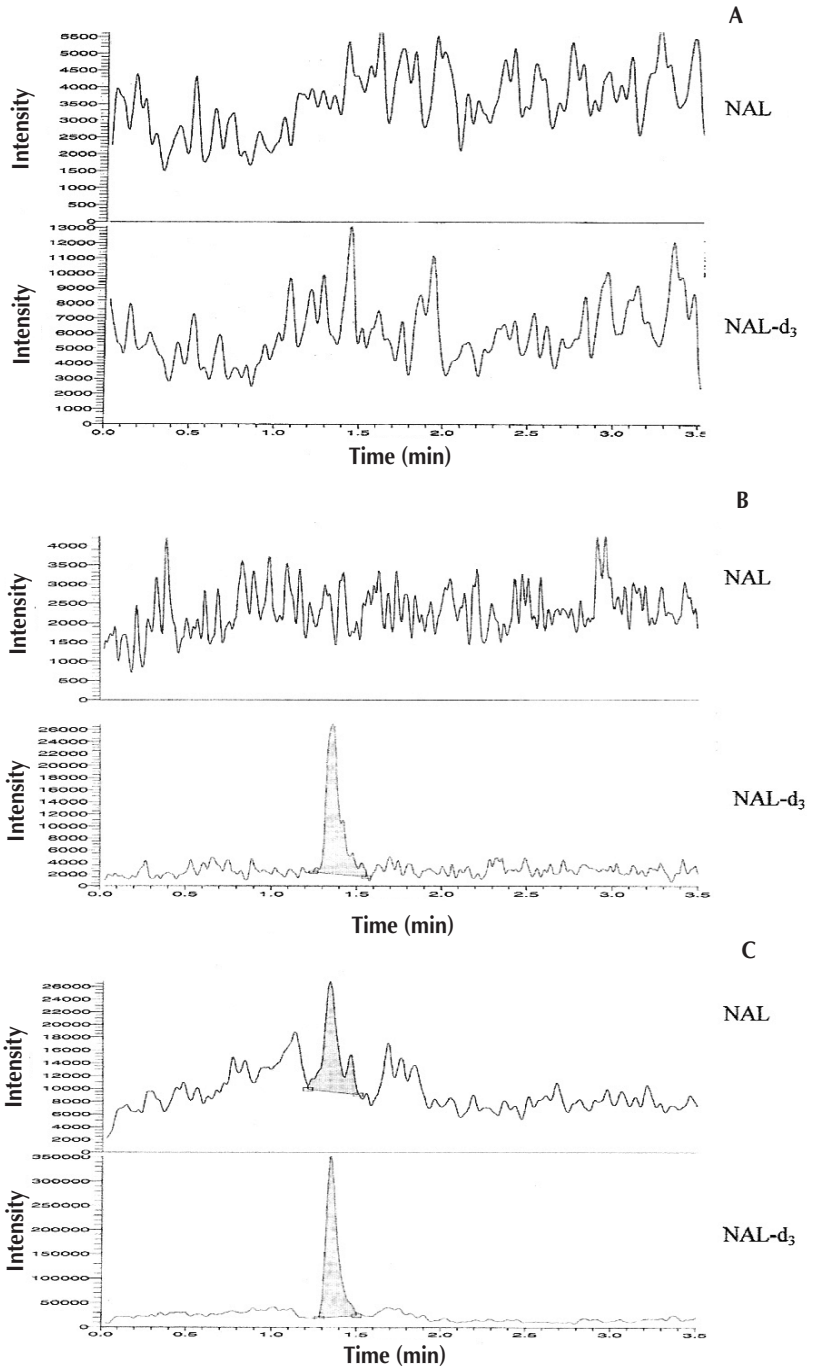

Figure 2. Representative chromatograms of blank (A), blank with internal standard (B), and a LOQ sample (C).

ever, for determination of NAL in the low pg/mL range in dog plasma. Therefore, to assess the pharmacokinetics of NAL in a pilot dog study, it was necessary to develop this method for analysis of plasma samples.

The use of stable isotope-labeled analogs as internal standards is highly recommended because similar relative efficiencies of ionization of the two molecular species would be expected to compensate for any matrix effect (18). In an effort to better understand the persistence of matrix effects in spite of the use of deuterated internal standards, we had earlier reported a molecular modeling approach to evaluate or predict isotope effects in a normal-phase chromatographic separation (19). Although column chromatography is a complex phenomenon involving several types of interactions, with relevance to deuterium isotope effect influencing resolution, we believe that analyte-stationary phase interactions would be the predominant factor. This is because chromatographic resolution of the deuterated and non-deuterated analogs under identical mobile phase conditions could have resulted mainly due to relative differences in analyte-stationary phase binding interactions. During molecular modeling, therefore, only these binding interactions were used for comparison.

In this study, it was decided to study NAL using a similar modeling approach as a means to evaluate whether or not an uncompensated matrix effect would be expected.

Experimental

Chemicals and reagents

Naltrexone hydrochloride (working standard) was obtained from Sigma (St. Louis, MO). [15,15,16-^{2}H]-naltrexone (NAL-d_3) was procured under license from the National Institute on Drug Abuse (NIDA, Rockville, MD) for use as an internal standard (IS). Figure 1 shows the structure of NAL. Analytical grades of formic acid, ammonium hydroxide and trifluoroacetic acid were purchased from Sigma. Methyl tert-butyl ether (MTBE) and HPLC grades of acetonitrile and methanol were purchased from Honeywell Burdick & Jackson (Muskegon, MI). Water was obtained in-house using the Nanopure Diamond water system (Barnstead International, Dubuque, IO).

Stock solution and stock dilution

Approximately 10 mg of working standard was accurately weighed and transferred into a 10-mL volumetric flask. It was dissolved in

methanol–water (50:50, v/v) to yield a stock solution, the exact concentration of which was corrected for NAL freebase. The stock solution was stored below 10°C in a refrigerator. A serial dilution was performed in the same solvent to yield stock dilutions ranging from 0.20 to 100.28 ng/mL, immediately prior to fortification into plasma.

Preparation of calibration curve and quality control standards

Dog plasma from two batches (containing sodium heparin as anticoagulant) was thawed and pooled to provide the matrix for the study. Spiking (5%, v/v) of the Stock Dilutions yielded calibration curve (CC) standards at 10, 25, 50, 100, 501, 1003, 2507, and 5014 pg/mL in the plasma. Similarly, quality control samples were prepared at 10, 29, 361 and 4512 pg/mL representing limit of quantitation (LOQ)-quality control (QC), low (LQC), middle (MQC) and high (HQC) controls, respectively. Aliquots were stored in capped tubes below –50°C until analysis. The storage duration was less than one week. Frozen plasma samples containing NAL are reported to be sufficiently stable (only 15% degradation observed after 576 days); hence, a detailed evaluation of stability was not conducted for the purpose of the pilot pharmacokinetic study (17,20).

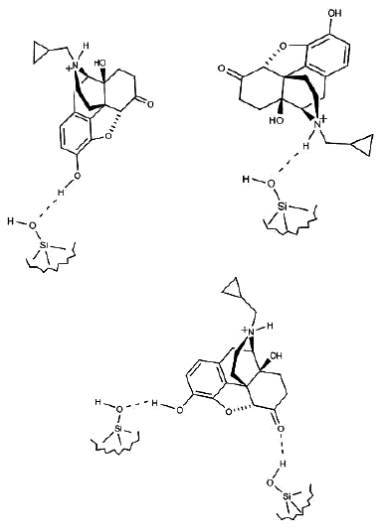

Figure 3. Representative positions of naltrexone interacting with the stationary phase.

Sample extraction

Prior to analysis, the CC standards and QC samples were thawed at room temperature. From each sample, 0.5 mL was transferred to a capped glass tube, and 10 µL of IS dilution (20 ng/mL of NAL-d_3) was added and vortex mixed. Five milliliters of ammonium hydroxide (0.6%, v/v) in MTBE was then added. Basic conditions were employed to maintain the analyte molecule in its non-ionized state, thereby preferentially partitioning the analyte into the organic phase. The samples were placed on a laboratory rotator and spun at 30 rpm for 15 min. After allowing approximately two min of standing to facilitate separation of the aqueous and organic phases, they were placed in a refrigerated circulator until the aqueous layer was frozen. The supernatant (organic layer) was poured into conical-bottomed tubes. These were evaporated to dryness at 50°C for 10 min under a stream of dry nitrogen at 10 psi. The residue was reconstituted in 100 µL of acetonitrile–water (50:50, v/v) and transferred into 200 µL silanized glass vials for analysis.

LC–MS–MS conditions

The Shimadzu *VP* LC system consisted of a system controller (SCL-10A), two high-pressure pumps (SIL-10AD, designated as Pumps A and B) and an autosampler (SIL-10AD) (Shimazdu, Kyoto, Japan). Chromatography was carried out using a Polaris Silica column (5 µm; 2.1 × 50 mm, purchased from Thermo-Electron, Inc., Waltham, MA). The reservoir of Pump A contained water with formic acid (1%, v/v) and trifluoroacetic acid (0.001%, v/v) added. Acetonitrile was employed as the reservoir of Pump B. The linear gradient employed at a flow rate of 0.35 mL/min is described in Table I. Acetonitrile–water (50:50, v/v) was used as a rinse solution for the injector, and the injection volume was fixed at 50 µL.

A TSQ 7000 triple-quadrupole mass spectrometer (Finnigan MAT, San Jose, CA) was used with Excalibur version 1.2 software for data acquisition and analysis. Electrospray ionization in the positive ion mode was employed. The multi-reaction monitoring transition at 342–324 for NAL was optimized for response and fixed at 345–327 for NAL-d_3.

The two transitions were confirmed for the absence of any "cross-talk" before subsequent optimization steps. This was

Table II. Reverse Predicted Concentration Residuals of Naltrexone

	Nominal concentration (pg/mL)								r^2	Slope	Intercept
Set #	10	25	50	100	501	1003	2507	5014			
1	10	23	54	95	502	1064	2165	5270	0.9880	0.0050	0.3067
2	12	27	45	98	451	979	2533	5143	0.9980	0.0216	0.1238
3	11	27	53	106	435	960	2275	5334	0.9923	0.0001	0.0168
Mean	11	25	51	100	463	1001	2325	5249			
SD	0.6	2.3	5.0	5.2	35.1	55.5	189.1	97.1			
CV (%)	5.6	9.2	9.8	5.3	7.6	5.5	8.1	1.9			
% nominal	108.9	101.5	101.9	99.7	92.4	99.8	92.7	104.7			

performed by infusion of a 1 µg/mL solution of one compound in methanol and checking for the absence of the other transition, and vice-versa. The same drug solution was infused for an iterative, manual optimization of other instrument parameters to the following values: Source, 5 kV; extractor, 37 V; manifold temperature, 70°C; and capillary temperature and voltage 275°C and 20 V, respectively. Nitrogen was used as the sheath gas at 70 psi, and purified air (zero grade), optimized to 2 mT, was employed in the collision cell.

A post-column infusion experiment was then conducted following the method of Bonfiglio et al. (21). A 10 ng/mL solution of NAL was prepared in acetonitrile–water (50:50, v/v), and was continuously infused at 5 µL/min into the mass spectrometer using a "tee", the third end of which was connected to the injector. Upon stabilization of the baseline response, a processed sample of blank dog plasma was injected, and the resulting profile was evaluated for any suppression of ionization.

Table III. Precision and Accuracy Data for Naltrexone

	Nominal Concentration (pg/mL)		
Set #	**29**	**361**	**4512**
	27	311	4989
1	25	309	4384
	34	375	3591
Mean	29	332	4321
SD	4.3	37.6	701.5
CV (%)	15.0	11.3	16.2
Nominal (%)	99.0	91.8	95.8
	23	369	4069
2	33	346	4719
	25	406	4103
Mean	27	374	4297
SD	5.2	30.3	365.7
CV (%)	19.2	8.1	8.5
Nominal (%)	93.6	103.5	95.2
	32	309	3952
3	30	320	4583
	35	302	4668
Mean	32	310	4401
SD	2.6	9.0	391.2
CV (%)	8.1	2.9	8.9
Nominal (%)	111.9	85.9	97.5
	Global calculation		
Mean	29	339	4340
SD	4.3	37.2	443.8
CV (%)	14.7	11.0	10.2
Nominal (%)	101.5	93.8	96.2

Table IV. A Comparison of Binding Energies of Naltrexone and [15,15,16-2H] Naltrexone*

Compound	Retention time (min)	Binding energy (kcal/mole)
Naltrexone	1.32 (0.01)	–10.22
[15,15,16-2H] Naltrexone	1.31 (0.01)	–10.26

* Values in parentheses represent standard deviation (n = 5).

Molecular modeling

Molecular modeling investigations were carried out using the approach described in our earlier work (19). An updated version of SYBYL version 7.2 was used. For modeling the deuterated analyte (NAL-d_3), the force constant and bond length parameters defining the C3 (sp^3 hybridized carbon)-D bond in the Tripos force field were modified to 800 and 1.075 Å, respectively, as opposed to 662.4 and 1.100 Å for the C3-H bond as reported previously. Furthermore, it was necessary to account for the charged, ionized state of the nitrogen at the 17th position at the pH of mobile phase. This was achieved in SYBYL by changing the hybridization state from N3 to N4. The two molecules were drawn and the energy minimized. Each analyte was rolled over the stationary phase surface and a three-dimensional visual examination was conducted to assess, qualitatively, the likelihood of analyte–stationary phase interactions. Twenty-five models were created in such a manner. Bond length constraints were applied for some positions of hydrogen bonds but were removed prior to the final energy minimization step. This was again followed by energy minimization of the resulting complexes to a gradient step-size of 0.05 kcal/mole. In Figure 3, representative positions of NAL interacting with the stationary phase are depicted. Finally, energy calculations were performed for each position as described in the following section.

Binding energy calculations

Energy calculations used the Tripos force field (22) in SYBYL. The total energy (E_{total}) for an arbitrary geometry of a molecule derived from a force field is given by the sum of energy contributions. For the Tripos force field, this can be represented as:

$$E_{total} = \Sigma E_{str} + \Sigma E_{bend} + \Sigma E_{oop} + \Sigma E_{tors} + \Sigma E_{vdw} + \Sigma E_{elec} + \Sigma E_{constraints} \quad \text{Eq. 1}$$

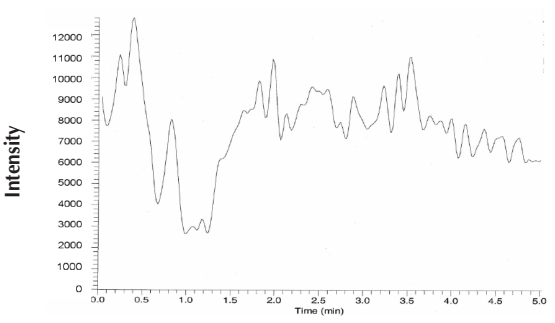

Figure 4. Ion suppression profile after post-column infusion of naltrexone.

where the sums extend all over the bonds, bond angles, torsion angles and non-bonded interactions between atoms not bound to each other or to a common atom, and where: E_{str} is the bond stretching energy term, E_{bend} is the angle bend energy term, E_{oop} is the out of plane bending energy term due to the bending of bonds from their natural values, E_{tors} is the torsional energy term due to the twisting of bonds, E_{vdw} is the Van der Waals energy term arising due to non-bonded interactions, E_{elec} is the electrostatic energy term, and $E_{constraints}$ is an energy term for the artificially inserted constraints (if any).

The Tripos force field treats the hydrogen bonds as non-directional and electrostatic in nature. To accommodate this, calculations in which hydrogen bonds are expected to be important include partial charges and the electrostatic contributions. Hydrogen bond energies are included in the evaluation of the force field by scaling the Van der Waals interactions between N, O, and F and hydrogens bonded to N, O, or F.

Thus, the binding energy (ΔE) for each position can be calculated as:

$$\Delta E = (E_{analyte} + E_{stationary\ phase}) - (E_{analyte\ +\ stationary\ phase}) \quad \text{Eq. 2}$$

where $E_{analyte}$, $E_{stationary\ phase}$, and $E_{analyte\ +\ stationary\ phase}$ represent the total energies of the free unbound analyte, unbound stationary phase and the bound analyte-stationary phase complex, respectively. During the calculation of average binding energy, any molecular model for analyte-stationary phase complexes that exhibited positive ΔE values were omitted from further consideration because these are not energetically possible.

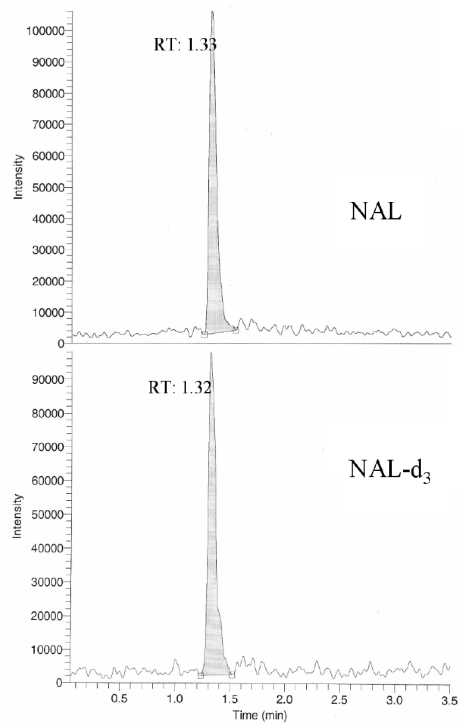

Figure 5. A representative chromatogram system suitability sample to demonstrate unresolved peaks for the drug and IS.

Results and Discussion

Figure 2 shows a representative chromatogram each of blank, blank with IS, and LOQ samples. The blank plasma sample was devoid of any interference at the retention time of NAL and IS. Also, no interference of NAL was observed from the IS in the blank sample fortified with IS. The post-column infusion experiment resulted in a relatively low amount (approximately 25%) of ion suppression at the retention time of the analyte (Figure 4). This indicated that optimal sample cleanup and chromatography had been achieved.

The calibration curves were linear in the range of 10–5014 pg/mL ($r^2 > 0.98$) using a weighting factor of 1/concentration. The concentration residuals were between 92.4–108.9% [relative standard deviation (RSD) = 1.9–9.8%]. The data are summarized in Table II. The LLOQ of the method was tested at 10 pg/mL by injection of plasma samples prepared and processed independent of the calibration curve. The deviation was found to be 9.8% of the nominal concentration (RSD = 4.8%, $n = 6$). The precision and accuracy of the method were calculated as the % RSD and percent of nominal value. The global interday precision and accuracy for three batches ($n = 9$) were found to be between 10.2–14.7%, and 93.8–101.5%, respectively (Table III).

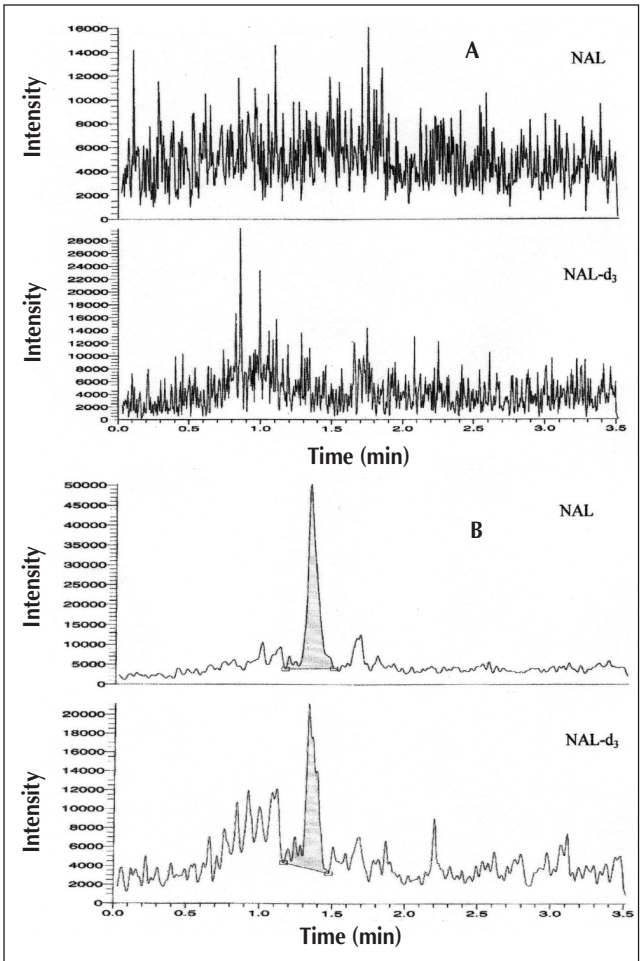

Figure 6. Chromatograms of pre-dose (A) and day 2 post-implantation dog samples (B).

The recovery of the method was determined by a comparison of peak heights of processed samples at the middle quality control level to the mean peak height of samples spiked at the same concentration level in reconstitution solution. The mean recovery was 40.9% (RSD = 1.3%; n = 5).

Immediately at the end of one of the analytical batches, a blank sample was injected to check for carry-over from the previous injection. The carry-over level was less than 5% of the mean peak height of the LLOQ indicating minimal binding of the analyte to exposed chromatographic surfaces and tubing.

The molecular models, created as described previously, were examined qualitatively for analyte–stationary phase interactions upon energy minimization. There are, in fact, nearly an infinite number of positions at which the analyte may have interactions with the stationary phase. One method of limiting the search, however, is to specify distance constraints between pairs of atoms. Assuming that a set of molecules presents a common range of distances between two particular molecular features that are chemically relevant, the search can be reduced to the exploration of the restricted conformational space defined by the acceptable range for this particular inter-atomic distance. For a hydrogen bond, this distance is between 1.7 Å and 2.3 Å. Different models of the bound analyte with the stationary phase revealed a different number and position of the hydrogen bonds. A few representative positions are shown in Figure 3. Out of 25 models created for NAL and NAL-d_3, four positions showed positive binding energies and were discarded as discussed in the previous section. The mean binding energies of the compounds along with their retention times are shown in Table IV and Figure 5. The calculated binding energy difference was found to be only 0.03 kcal/mole; thus, it is expected that the two analytes should not exhibit different retention behaviors in the column. This calculation is consistent with the experimental observation.

Furthermore, upon a comparison of binding energy difference and chromatographic resolution of the isotopologs of NAL, olanzapine, and des-methyl olanzapine [the latter two analytes had been employed in our earlier study (19)], it was found that NAL had the lowest value for binding energy difference, a trend consistent with the resolution obtained experimentally. The data with a linear relationship are represented in Table V and Figure 7. Although both olanzapine and NAL have three hydrogen atoms substituted for deuterium, the major difference lies in the presence of a quaternary nitrogen in NAL and the clustering of deuterium atoms near the charged nitrogen. These results are consistent with the findings of Zhang et al. (23). Studies with deuterium substituted analogs with deuterium atoms at multiple positions will be necessary to further validate this approach; nevertheless, it is speculated that during development of quantitative LC–MS–MS methods, the number and position of deuterium atoms on an isotopically labeled internal standard needs consideration for its ability to compensate for any matrix effect.

Application to a pilot implantation study in dog

The analytical method was employed for the analysis of dog plasma samples collected from a pilot study involving subcutaneous implantation of a biodegradable dosage form of NAL. The pre-dose plasma sample showed no interference at the retention time of NAL and NAL-d_3 and the chromatogram of the day 2 sample is shown in Figure 6.

Conclusion

The LC–MS–MS method has been shown to be selective, sensitive, accurate, and precise for the quantitation of NAL in dog plasma samples. It involves a simple, single step extraction procedure and, therefore, is easily applicable to routine preclinical sample analyses. For pivotal studies however, a more comprehensive validation would be required.

Additional information obtained through molecular modeling provides a useful, semi-quantitative understanding of analyte-stationary phase interactions. The binding energies calculated from the models explain the identical retention times of the deuterated and non-deuterated analogs observed experimentally. Further molecular modeling studies on a series of internal standards that have different number and positions of isotopic substitutions are necessary to create a basis for their selection in quantitative LC–MS–MS analyses.

Acknowledgements

The authors thank the Bioanalytical Core Laboratory, VCU School of Pharmacy for LC–MS–MS instrumentation and supplies, and the VCU Institute for Structural Biology and Drug Discovery, Virginia Biotechnology Research Park, Richmond, VA for molecular modeling facilities.

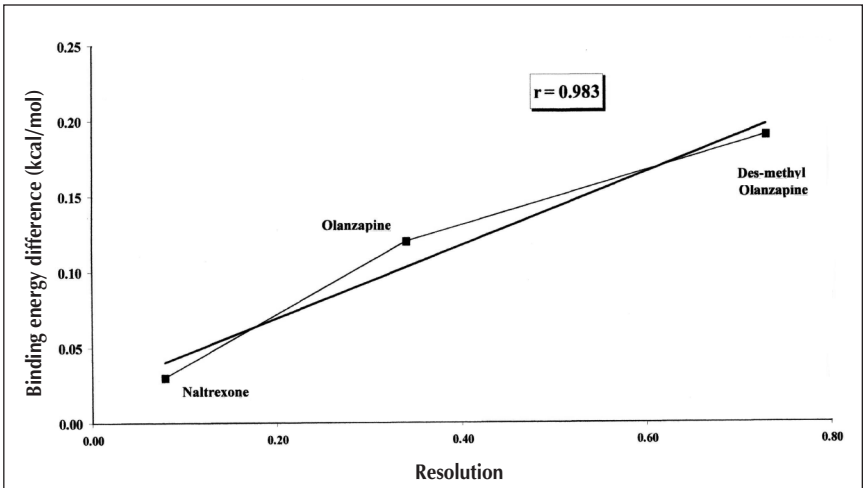

Figure 7. Linear relationship of the binding energy difference between isotoplogs to their chromatographic resolution.

References

1. J.P. Gonzalez and R.N. Brogden. Naltrexone: a review of its pharmacodynamic and pharmacokinetic properties and therapeutic efficacy in the management of opioid dependence. *Drugs* **35:** 192–213 (1988).
2. J.R. Volpicelli, A.L. Alterman, M. Hayashida, and C.P. O'Brian. *Arch. Gen. Psychiatry* **49:** 876–80 (1992).
3. S. O'Malley, A.J. Jaffe, G. Chang, R.S. Scottenfeld, R.E. Meyer, and B. Rounsaville. *Arch. Gen. Psychiatry* **49:** 881–87 (1992).
4. T.L. Mark, H.R. Kranzler, and X. Song. Understanding US addiction physicians' low rate of naltrexone prescription. *Drug Alcohol Depend.* **71:** 219-28 (2003).
5. A.L. Stinchcomb, P.W. Swaan, O. Ekabo, K.K. Harris, J. Browe, D.C. Hammel, T.A. Cooperman, and M. Pearsall. Straight-chain naltrexone ester prodrugs: diffusion and concurrent esterase biotransformation in human skin. *J. Pharm. Sci.* **91:** 2571–78 (2002).
6. S.D. Comer, E.D. Collins, H.D. Kleber, E.S. Nuwayser, J.H. Kerrigan, and M.W. Fischman. Depot naltrexone: long-lasting antagonism of the effects of heroin in humans. *Psychopharmacology* **159:** 351–60 (2002).
7. R.T. Bartus, D.F. Emerich, J. Hotz, M. Blaustein, R.L. Dean, B. Perdomo, and A. S. Basile. Vivitrex®, an injectable, extended-release formulation of naltrexone, provides pharmacokinetic and pharmacodynamic evidence of efficacy for 1 month in rats. *Neuropsychopharmacology* **28:** 1973–82 (2003).
8. *Narcotic Antagonists: Naltrexone pharmacochemistry and sustained-release preparations;* Research Monograph Series No. 28 Part II; National Institute on Drug Abuse, U.S. Department of Heath and Human Services, U.S. Government Printing Office: Washington, DC, 1981.
9. K.K. Peh, N. Billa, and K.H. Yuen. Simple liquid chromatographic method for the determination of naltrexone in human plasma using amperometric detection. *J. Chromatogr., B* **701:** 140–45 (1997).
10. W.J. Hurst, I.S. Zagon, and H.Y. Aboul-Enein. A rapid sample preparation method for the HPLC determination of opioid antagonist naltrexone in serum. *Pharmazie* **54:** 595–96 (1999).
11. K. Kambia, S. Bah, T. Dine, R. Azar, P. Odou, B. Gressier, M. Luyckx, C. Brunet, L. Ballester, M. Cazin, and J.C. Cazin. High-performance liquid chromatographic determination of naltrexone in plasma of hemodialysis patients. *Biomed. Chrom.* **14:** 151–55 (2000).
12. Online website: http://www.lowdoesnaltrexone.org (May 8, 2006).
13. M.C. Lee, H.N. Wagner Jr., S. Tanada, J.J. Frost, A.N. Bice, and R.F. Dannals. Duration of occupancy of opiate receptors by naltrexone. *J. Nucl. Med.* **29:** 1207–11 (1988).
14. C.F. Chan, G.M. Chiswell, R. Bencini, L.P. Hackett, L.J. Dusci, and K.F. Ilett. Quantification of naltrexone and 6β-naltrexol in plasma and milk using gas chromatography-mass spectrometry: Applications to studies in lactating sheep. *J. Chromatogr. B* **761:** 85–92 (2001).
15. K.M. Monti, R.L. Foltz, and D.M. Chinn. Analysis of naltrexone and 6-beta-naltrexol in plasma and urine by gas chromatograph/negative ion chemical ionization mass spectrometry. *J. Anal. Toxicol.* **15:** 136–40 (1991).
16. W. Naidong, H. Bu, Y.L. Chen, W.Z. Shou, X. Jiang, and T.D.J. Halls. Simultaneous development of six LC-MS-MS methods for the determination of multiple analytes in human plasma. *J. Pharm. Biomed. Anal.* **28:** 1115–1126 (2002).
17. C.J.L. Buggé, I.U. Grün, K. Stanford, M.S. Tan, and D.B. Garcia. *Determination of naltrexone and 6β-naltrexol in human plasma by LC–MS–MS;* Cedra Corporation: Austin, TX, 1996.
18. C.M. Chavez-Eng, M.L. Constanzer and B.K. Matuszewski. High-performance liquid chromatographic–tandem mass spectrometric evaluation and determination of stable isotope labeled analogs of rofecoxib in human plasma samples from oral bioavailability studies. *J. Chromatogr., B* **767:** 117–29 (2002).
19. S.S. Iyer, Z.-P. Zhang, G.E. Kellogg, and H. Thomas Karnes. Evaluation of deuterium isotope effects in normal-phase LC-MS-MS separations using a molecular modeling approach. *J. Chrom. Sci.* **42:** 383–87 (2004).
20. D.E. Moody, K.M. Monti, A.C. Spanbauer, and J.P. Hsu. Long-term stability of abused drugs and antiabuse chemotherapeutical agents stored at –20°C. *J. Anal. Toxicol.* **23:** 535–40 (1999).
21. R. Bonfiglio, R.C. King, T.V. Olah, K. Merkle. The effects of sample preparation methods on the variability of the electrospray ionization response for model drug compounds. *Rapid Commun. Mass Spectrom.* **13:** 1175–85 (1999).
22. *Force Field Manual*; Version 6.6, Chapter 3; Tripos Inc.: St. Louis, MO, 1999; p 81.
23. R. Zhang, C.S. Sioma, R.A. Thompson, L. Xiong, and F.E. Regnier. Controlling deuterium isotope effects in comparative proteomics. *Anal. Chem.* **74:** 3662–69 (2002).

Manuscript received June 26, 2006;
revision received February 12, 2007.